

# Preliminary Study of Motion Artifact Rejection for NIBP measurement in an Ambulance

Yoonseo Koo, Jaemin Kang, Il Hyung Shin, Min Yang Jung, Gil Joon Suh, and Hee Chan Kim, *Member  
IEEE*

**Abstract**— Motion artifact resulting from patient’s movement is a significant source for disturbing accurate noninvasive blood pressure (NIBP) measurement. In an ambulance, patients are exposed to unstable circumstances due to vehicle’s movement and vibration during emergency transportation. Since NIBP is indirectly measured using oscillometry based on the change of cuff pressure, it can be affected by motion artifact much more than other biosignals. In this paper, we developed a new NIBP system with improved accuracy by measuring acceleration of the system caused by patient’s motion. The NIBP module including a 3-axis accelerometer was directly mounted on a cuff to minimize the interference induced through connecting tube. The results show that the proposed NIBP system has the capability to reject the interference of motion artifact effectively in an ambulance.

## I. INTRODUCTION

Blood pressure is one of the fundamental biological signals in monitoring patient’s health state. The most popular way to measure the noninvasive blood pressure (NIBP) is the oscillometric method. However, NIBP measurement is highly vulnerable to motion artifact, such as patient’s movement, talking and coughing that leads to degrade the accuracy of measurement [1], [2]. In emergency situation, especially in an ambulance, patients are exposed to more difficult circumstances for measuring accurate NIBP because of vehicle’s movement on the road as well as mechanical vibration. Many studies have proposed several techniques to reduce the interference of motion artifact and improve the accuracy of NIBP measurement. The

frequency-domain filtering methods or Kalman filter were generally applied to reject the motion artifact [3-5]. However, since the frequency bandwidth of motion artifact overlaps with the oscillometric signal, it is not easy to reject the effect of the motion artifact successfully. Pulse matching algorithm that uses the pattern matching of beat pulses was also proposed to reject motion artifact [6], [7]. This method used fuzzy theory or a regression model algorithm to discriminate abnormal pulses from the normal ones. However, because these previous methods are basically post-processing algorithms, they are ineffective for large and random interferences easily involved during ambulance transportation. In this paper, we measured acceleration together with oscillometric signal in a newly developed NIBP module mounted on a cuff. Then an algorithm based on the measured acceleration was applied to reject the interference resulting from motion artifact. The performance of the developed system was also verified through simulated experiments and the results show that the developed NIBP system is practical for rejecting the interference of motion artifact.

## II. MATERIALS AND METHODS

### A. Measurement Module Description

Our research group has developed a prototype system of Ubiquitous Integrated Biotelemetry System for Emergency Care (UIBSEC) [8] to be used by emergency rescuers to get directions from medical doctors in providing emergency medical services for patients in ambulance. Fig. 1 shows the developed NIBP module for rejecting the interference of motion artifact to be used in UIBSEC. There are two differences between the new module and the existing one. First, the length of the tube which is connected between the cuff and instrument was minimized in the new module. The interference induced in the connecting tube is another source of motion artifact. Thus, we minimized the length of the tube by developing a small size module to be directly mounted on the cuff. To make the NIBP module small, circuitry having low power consumption was designed. Small motor-driven air pump and solenoid valve were also used. The dimension of the developed NIBP module is 50mm x 80mm x 20mm. Secondly, we used a 3-axis accelerometer to calculate and reject the interfered pressure by measuring the acceleration on the cuff. The block diagram of the developed NIBP module was shown in Fig. 1.

Manuscript received April 16, 2007. This work was supported by the Korea Science and Engineering Foundation (KOSEF) grant funded by the Korea government (MOST) (No. M10536060001-06N3606-00110)

Yoonseo Koo is with Interdisciplinary Program, Biomedical Engineering Major, Graduate School, Seoul National University, Seoul, Korea (email: kattack9@melab.snu.ac.kr).

Jaemin Kang is with Interdisciplinary Program, Biomedical Engineering Major, Graduate School, Seoul National University, Seoul, Korea (email: jmkang@melab.snu.ac.kr).

Il Hyung Shin is with Interdisciplinary Program, Biomedical Engineering Major, Graduate School, Seoul National University, Seoul, Korea (email: lepagats@melab.snu.ac.kr).

Min Yang Jung is with Interdisciplinary Program, Biomedical Engineering Major, Graduate School, Seoul National University, Seoul, Korea (email: minyang@melab.snu.ac.kr).

Gil Joon Suh is with Department of Emergency Medicine, Seoul National University, Seoul, Korea (email: suhgil@snu.ac.kr).

Hee Chan Kim is with Department of Biomedical Engineering, College of Medicine and Institute of Medical and Biological Engineering, Medical Research Center, Seoul National University, Seoul, Korea (email: hckim@snu.ac.kr).

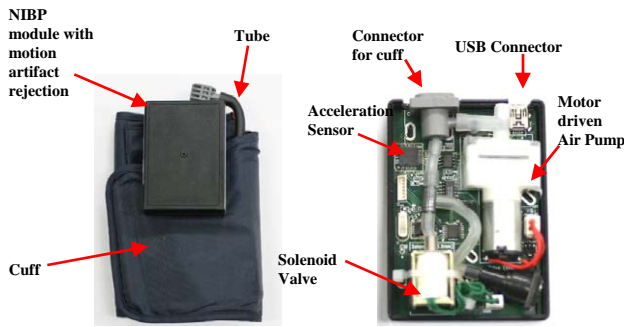


Fig. 1. NIBP module and block diagram for rejecting motion artifact

### B. Algorithm

Fig. 2 illustrates the NIBP measurement in an ambulance. NIBP measurement is conducted on a patient lying on an emergency bed and wearing the module as shown in Fig. 2. In this case, measured pressure ( $P_m(t)$ ) is the addition of cuff pressure without the motion artifact ( $P_c(t)$ ) and the pressure interfered by motion ( $P_a(t)$ ).

$$P_m(t) = P_c(t) + P_a(t). \quad (1)$$

Thus, the main idea of rejecting motion artifact is to calculate  $P_c(t)$  by subtracting  $P_a(t)$  from the measured  $P_m(t)$ .  $P_a(t)$  is calculated by using measured acceleration ( $a(t)$ ) and can be considered as an output of the system having transfer function ( $H(s)$ ) for  $a(t)$ . Though it should be computed using accurate  $H(s)$  via system modeling, we constructed  $P_a(t)$  using trials and errors based on repetitive experiments. Finally,  $P_a(t)$  is calculated by using a combination of low pass filter and gain control.

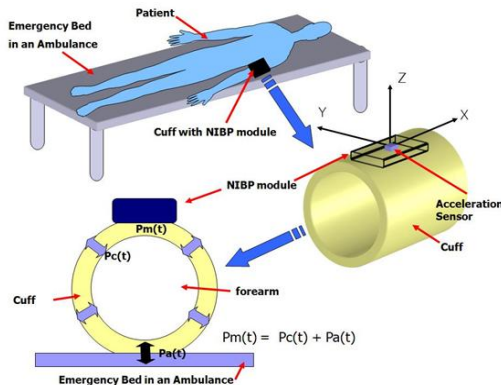


Fig. 2. NIBP module with motion artifact rejection in an ambulance

The experiment was conducted as follows. We wrapped the cuff around the cylindrical object whose radius, height and weight are known. Then, we applied pressure to the cuff up to a certain pressure value (150mmHg) and stopped. In the decompression process, we purposely made motion artifact by moving the cylindrical object. After this process, using NIBP simulator (SmartArm™, Clinical Dynamics Corporation, U. S. A.), the proposed algorithm was applied to the blood pressure patterns with motion artifact. Fig. 3 shows the measured raw data, which are cuff pressure and acceleration on each axis.

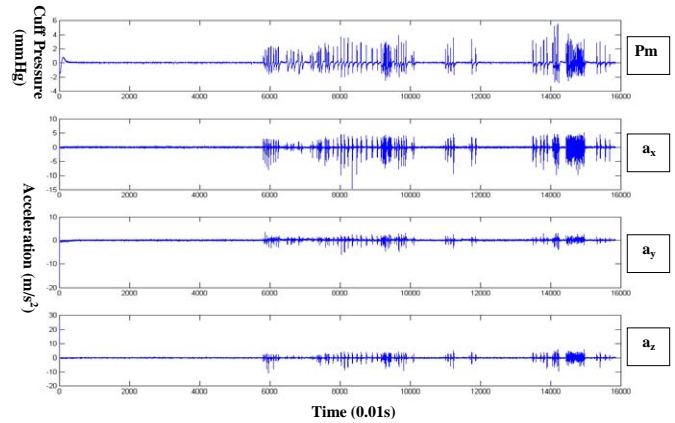


Fig. 3. Measured raw data

As shown in Fig. 3,  $P_m(t)$  has a similar pattern to that of acceleration. Motion artifact rejection algorithm shown in Fig. 4 was applied to the measured data. We determined the algorithm to construct  $P_a(t)$  close to the measured motion artifact  $P_m(t)$  using simultaneously measured  $a(t)$ .  $P_m(t)$  was calculated from raw pressure data using band-pass filter.  $a(t)$  was calculated from the vector sum of 3-axis acceleration signals, and then was transformed into scalar form.  $a(t)$  was divided into positive and negative signals. After the divided signals went through a low-pass filter, they were multiplied by gain factors  $G_p$  and  $G_n$ , respectively. Finally, the two processed signals were added to construct  $P_a(t)$ . The cutoff frequency of low-pass filter and gain factors were determined by minimizing  $E = \text{MAX}(P_m(t) - P_a(t))$ . The determined cutoff frequencies for each low-pass filter were 6Hz and 3Hz, and the gain factors were  $G_p = 12.6$  and  $G_n = 15$ , respectively.

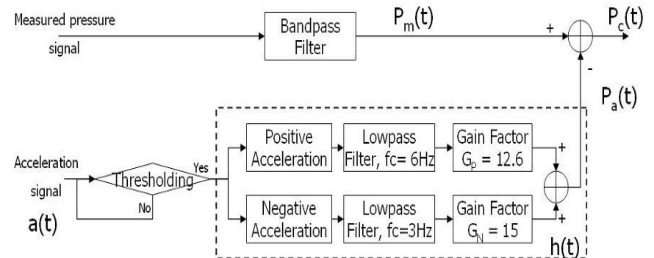


Fig. 4. Flowchart of motion artifact rejection algorithm using acceleration

As shown in Fig. 5,  $P_a^+(t)$  and  $P_a^-(t)$ , which were processed as mentioned above, generates constructed pressure  $P_a(t)$  caused by motion. The pattern of  $P_a(t)$  shows similarity to that of  $P_m(t)$ , which is the actual measured pressure. Fig. 6 shows  $P_c(t)$  obtained by subtracting  $P_a(t)$  from real motion artifact

$P_m(t)$ .  $P_c(t)$  has some ripple amplitude because of the limitation of the current model.

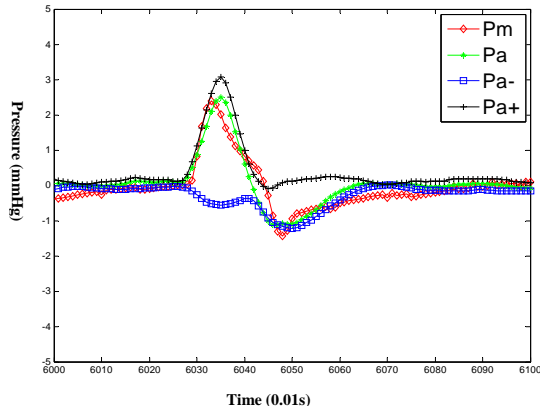


Fig. 5. Calculated  $P_a(t)$  from algorithm

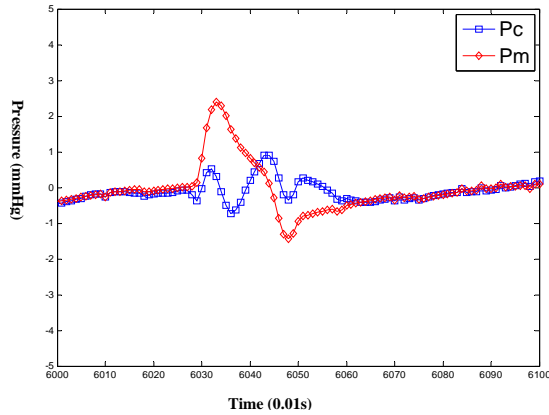


Fig. 6.  $P_m(t)$  and motion artifact rejected  $P_c(t)$

### III. RESULTS

The amplitude comparison between peaks of real motion artifact  $P_m(t)$  and those of constructed  $P_a(t)$  was performed to evaluate the performance of proposed algorithm, and the resulting data were drawn in Fig. 7. We can confirm that the peak amplitude level of  $P_a(t)$  is similar to that of  $P_m(t)$ . The slope of regression model is approximately 0.96.

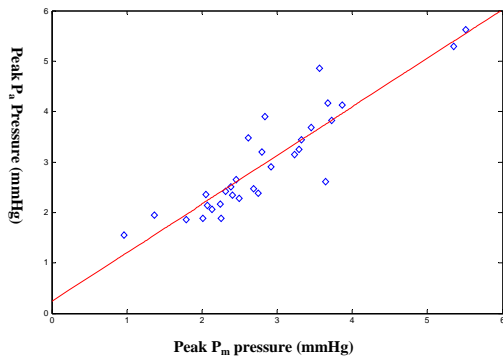


Fig. 7. Amplitude comparison with real motion artifact pressure  $P_m(t)$  and constructed motion artifact pressure  $P_a(t)$

Table I shows a summary of results for  $P_c(t)$  which is calculated by the algorithm using measured motion artifact  $P_m(t)$  and constructed motion artifact  $P_a(t)$ .

Table I. Real pressure  $P_m(t)$  and Constructed pressure  $P_a(t)$

	Construction ratio (N=30)	Correlation coefficient (N=30)	Ripple amplitude (mmHg) (N=30)	Ripple ratio (N=30)
Mean	1.0653	0.9079	0.6314	0.3079
Std	0.1859	0.0364	0.2339	0.0895

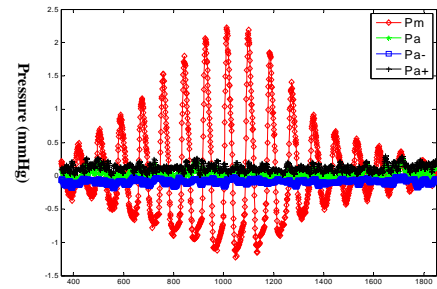
Construction ratio = max amplitude of  $P_a(t)$  / max amplitude of  $P_m(t)$

Correlation coefficient = correlation coefficient of  $P_a(t)$  and  $P_m(t)$

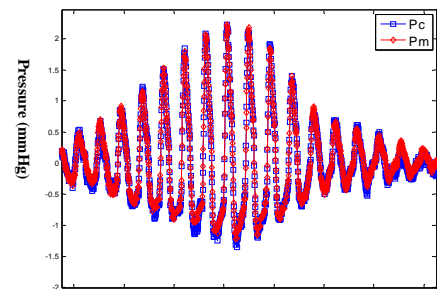
Ripple amplitude = max amplitude of  $P_c(t)$

Ripple ratio = max amplitude of  $P_c(t)$  / max amplitude of  $P_m(t)$

As shown in the result,  $P_a(t)$  is constructed as having a similar peak amplitude level with that of  $P_m(t)$ . And the correlation coefficient of  $P_a(t)$  and  $P_m(t)$  was 0.9. However, when performing the subtraction of  $P_a(t)$  from  $P_m(t)$ , ripples are produced because the two patterns are not exactly matched. Nevertheless, it is possible to reject the peak of the motion artifact to 70% on average, and the result is shown in the fourth column of Table 1. Thus, the developed NIBP module and the proposed algorithm were applied to the blood pressure patterns using NIBP simulator. Fig. 8 and 9 show the results. Measured cuff pressure  $P_m(t)$  without motion artifact and  $P_a(t)$  constructed from acceleration are shown in Fig. 8(a). Fig. 8(b) shows  $P_c(t)$  obtained by subtracting  $P_a(t)$  from  $P_m(t)$ .  $P_a(t)$  was vaguely shown without motion artifact. Thus, we can find that the motion artifact-rejected  $P_c(t)$  signal is very similar to measured  $P_m(t)$ . Fig. 9 shows the graph with motion artifact. Time intervals of 100~110 sec and 115~125 sec, where motion artifact occurred are shown in Fig. 9(a).



(a)  $P_m(t)$  and  $P_a(t)$



(b)  $P_m(t)$  and  $P_c(t)$

Fig. 8. Measured graph without motion artifact

We can find that motion artifacts were rejected in enlarged intervals as shown in Fig. 9(b) and (c).

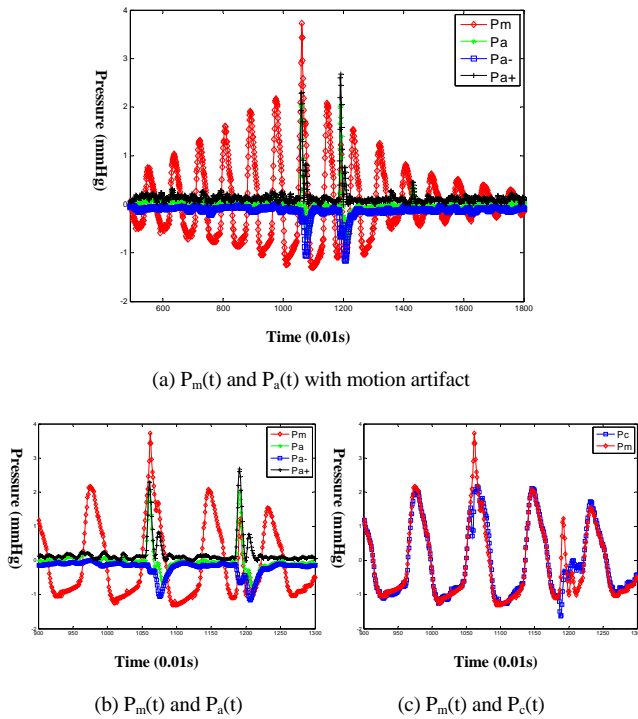


Fig. 9. Measured graph with motion artifact

#### IV. CONCLUSION

In this study, we developed a new NIBP module to reject the interference of motion artifact. The information of patient's movement is inferred from calculated acceleration. Using this acceleration data, we attempted to remove the interference in NIBP. The cuff pressure caused by motion was calculated through trials and errors experiments for preliminary study. In the results, we have found the possibility to reject the interference of motion artifact efficiently using acceleration. However, the proposed algorithm shows only limited achievement because it was not based on exact modeling of the cuff pressure. The modeling of cuff pressure caused by motion can be a solution to overcome these current limitations. The study using previous signal processing methods with proposed algorithm can also be another solution. Therefore, we should make experiments in various situations in an ambulance. The data obtained through the experiments will be used for exact modeling of cuff pressure caused by motion. The frequency-domain analysis of NIBP with acceleration, such as Short-Time Fourier Transform will be also used to improve accuracy of NIBP measurement.

#### REFERENCES

[1] R.N. Van Horn, R.J. Kahlke, L.A. Taylor, and T.J. Dorsett, "Noninvasive blood pressure performance: a reproducible method for

quantifying motion artifact tolerance in oscillometry", *Biomed Instrum Technol*, vol.35, pp.395-41, 2001

[2] Yu.G. Sterlin, A.N. Rogoza, L.Sh. Rozenblat, V.V. Balakin, and S.B. Nemirovskii, "Methods for increasing reliability and noise protection of arterial pressure measurement channel", *Biomedical Engineering*, vol.39, no.4, pp.167-173, 2005. *Translated from Meditsinskaya Tekhnika*, vol.39, no.4, pp.18-24, 2005.

[3] T.J. Dorsett and C.L. Davis, "Method of artifact rejection for noninvasive blood-pressure measurement by prediction and adjustment of blood- pressure data", U.S. Patent No.4949710, 1990

[4] R.G. Bennett and L.A. Taylor, "Arrhythmia compensation of a predictive noninvasive blood pressure algorithm", *Proceedings of Annual International Conference of the IEEE EMBS*, vol.13, no.5, pp.2114-5, 1991.

[5] L.A. Taylor, R.G. Bennett and T.J. Dorsett, "The application of signal averaging to the NIBP oscillometric waveform", *Proceedings of Annual International Conference of the IEEE EMBS*, vol.1, pp.691-2, 1995

[6] CT Lin, SH Liu, JJ Wang, and ZC Wen, "Reduction of interference in oscillometric arterial blood pressure measurement using fuzzy logic", *IEEE transactions on Biomedical Engineering*, vol.50, no.4, pp.432-41, 2003.

[7] C Huo, J Wang, J Zhang, and S Liu, "Blood pressure measurement based on wavelet analysis and fuzzy inference method", *Proceedings of the 6th World Congress on Intelligent Control and Automation*, vol.1, pp.4382-6, 2006

[8] Jaemin Kang, Honggu Chun, Il Hyung Shin, Sang Do Shin, Gil Joon Suh and Hee Chan Kim, "Preliminary evaluation of the use of a CDMA-based emergency telemedicine system", *Journal of Telemedicine and Telecare*, Vol.12, No.8: pp.422-427, 2006